Available online at http://scik.org
Eng. Math. Lett. 2019, 2019:2
https://doi.org/10.28919/eml/3908
ISSN: 2049-9337

SPECTRA OF OPERATORS ASSOCIATED WITH FLOW AROUND AN INFINITE CYLINDER

JONATHAN GUSTAFSSON[1], SIVAGURU S. SRITHARAN[2,*]

[1]Department of Mathematics & Statistics, Air Force Institute of Technology, Dayton, OH 45433, USA

[2]Office of the Provost & Vice Chancellor, Air Force Institute of Technology, Dayton, OH 45433, USA

Abstract. Numerical approximations of the spectrum of the Oseen operator and the spectrum of the linearised Navier–Stokes operator for flow around a cylinder in two dimensions have been studied for Reynolds numbers in the range 2 to 40. By using a spectral method featuring basis functions covering the entire exterior domain, it is possible to obtain a numerical approximation to the continuous spectrum and the point spectrum. The numerical approximation of the spectra seems to agree with the expected rigorous results. Namely a parabolic tongue containing the continuous spectra for the Oseen operator and for the linearised Navier–Stokes operator a parabolic tongue containing the continuous part of the spectrum plus a finite number of isolated eigenvalues.

Keywords: spectra of operators; infinite cylinder; Oseen operator; Navier–Stokes operator.

2010 AMS Subject Classification: 34K08.

*Corresponding author

E-mail address: Sivaguru.Sritharan@afit.edu

Received September 24, 2018

1. Introduction

Flow around an infinite cylinder in an unbounded domain with the fluid at infinity moving at prescribed velocity parallel with the x–axis, $\mathbf{e}_x$, is an archetypical problem in fluid mechanics. The flow will have different families of solutions depending on the Reynolds number. Low Reynolds number will lead to two dimensional laminar flow. For high Reynolds number, the flow will be turbulent and three dimensional. For physical experiments from flow around cylinders, Taneda [27], Gerrard [13], and Coutanceau and Bouard [8].

By linearised Navier–Stokes operator, we mean a *small* perturbation around a solution to the steady Navier–Stokes system. This method of linear stability theory has been applied to many different flows, see Chandrasekhar [7]. Most famous are the Bénard problem, Lord Rayleigh O.M. F.R.S. [21] and Rayleigh Taylor instability, Lord Rayleigh O.M. F.R.S. [20]. Nonlinear stability analysis and bifurcation theory also rely on spectral structure of these linearised operators, see Babenko [2], Drazin [10], Yudovich [28], Sritharan [26] and Schmid and Henningson [25].

The linearised spectrum, in particular a careful computation of the discrete and continuous spectrum is essential for the understanding of onset of periodic solutions (Karman vortex shedding) due to the crossing of discrete spectra as Reynolds number is increased. Feedback control of hydrodynamic stabilities require identification of the location of the spectrum so that suitable feedback compensators can be defined to stabilize the unstable modes by moving the unstable eigenvalues to the left by control action. This is particularly true when robust feedback control methods such as H^∞ control techniques are utilized. Hence the computational methods developed in this paper provide an essential step in robust feedback control of hydrodynamic instabilities from stationary solutions.See Barbu and Sritharan [4] and Park et al. [18].

The spectrum of the linearised NavierStokes operator in two dimensions for flows past a compact body has previously been studied both from a analytic viewpoint, [see 24, 3, 11] and numerically [see 15, 29]. Jackson [15] and Zebib [29] focused on numerically finding the first eigenvalues corresponding to periodic solutions. This was done to investigate the transition from steady to periodic solutions. Jackson [15] used a finite element method and Zebib [29] used a Chebyshev polynomials based spectral method. Both articles used domain truncation.

Note that domain truncation fundamentally changes the character of the spectrum. In bounded domain the linearised operators only has isolated eigenvalues, see also Davies [9], Sattinger [24] and Richtmyer [23]. In this article we present a spectral method with a basis covering the entire exterior. This spectral method was used to numerically approximate both the continuous part of the spectrum and the isolated eigenvalues. The pseudo-spectra of the Orr-Sommerfeld operator was numerically calculated by Reddy et al. [22]. In Jackson [15] or Zebib [29], only eigenvalues corresponding to the transition between stationary and non-stationary flow were computed.

In order to find the spectrum of linearised Navier–Stokes operator, a known solution to the steady Navier–Stokes system is needed. The spectral problem is obtained as a perturbation to the solution to steady Navier–Stokes system. We consider viscous, incompressible flow around an infinite cylinder. Denoting Ω as the domain exterior to the unit disc, the Navier–Stokes system for this case is, with $\mathbf{x} = (x, y, z)$ in Ω and $t > 0$,

$$\left(\frac{\partial}{\partial t} + w\cdot\nabla - \frac{1}{Re}\nabla^2\right) w + \nabla p = \mathbf{0}, \qquad x \in \Omega, t > 0, \tag{1a}$$

$$\nabla \cdot w = 0, \qquad x \in \Omega, t > 0, \tag{1b}$$

$$w(\mathbf{x}, 0) = \bar{\mathbf{g}}(\mathbf{x}), \qquad x \in \Omega, \tag{1c}$$

$$\text{on the boundary } w(\mathbf{x}, t) = \mathbf{0}, \qquad x \in \partial\Omega, t > 0 \tag{1d}$$

$$\text{and far field condition } \lim_{|\mathbf{x}|\to\infty} w(\mathbf{x}, t) = \mathbf{e}_x \qquad t > 0. \tag{1e}$$

Here w is the velocity field, p is the pressure field, and Re is the Reynolds number based on the diameter of the cylinder. The unit vector in x–direction is denoted $\mathbf{e}_x$. On the surface of the cylinder no–slip condition is applied. The initial velocity field is $\bar{\mathbf{g}}(\mathbf{x})$. To transfer the prescribed velocity from infinity to the cylinder, we will use the following transformation,

$$w = V + \mathbf{e}_x, \tag{2}$$

and arrive at the following system. For $\mathbf{x} \in \Omega$ and $t > 0$,

$$\left(\frac{\partial}{\partial t} + V \cdot \nabla - \frac{1}{Re}\nabla^2 + \frac{\partial}{\partial x}\right) V + \nabla P = \mathbf{0}, \qquad x \in \Omega, t > 0, \tag{3a}$$

$$\nabla \cdot V = 0, \qquad x \in \Omega, t > 0, \tag{3b}$$

$$V(\mathbf{x}, 0) = \mathbf{g}(\mathbf{x}), \qquad x \in \Omega, \tag{3c}$$

$$\text{on the boundary } V(\mathbf{x}, t) = -\mathbf{e}_x, \qquad x \in \partial\Omega, t > 0, \tag{3d}$$

$$\text{and far field condition } \lim_{|\mathbf{x}| \to \infty} V(\mathbf{x}, t) = \mathbf{0}, \qquad t > 0. \tag{3e}$$

Let us denote the solution to steady Navier–Stokes system (3) as $(\bar{v}, \bar{p})$ and perturb the full system around this solution:

$$V(t) = \bar{v} + v(t), \quad P(t) = \bar{p} + p(t). \tag{4}$$

The perturbed system, would be

$$\left(\frac{\partial}{\partial t} - \frac{1}{Re}\nabla^2 + \frac{\partial}{\partial x}\right) v + (v \cdot \nabla) v + \nabla p$$

$$+ (v \cdot \nabla)\bar{v} + (\bar{v} \cdot \nabla) v = \mathbf{0}, \qquad x \in \Omega, t > 0, \tag{5a}$$

$$\nabla \cdot v = 0, \qquad x \in \Omega, t > 0, \tag{5b}$$

$$v(\mathbf{x}, 0) = \mathbf{g}'(\mathbf{x}), \qquad x \in \Omega, \tag{5c}$$

$$\text{on the boundary } v(\mathbf{x}, t) = \mathbf{0}, \qquad x \in \partial\Omega, t > 0, \tag{5d}$$

$$\text{and far field condition } \lim_{|\mathbf{x}| \to \infty} v(\mathbf{x}, t) = \mathbf{0}, \qquad t > 0. \tag{5e}$$

The system (5) is rewritten as

$$\frac{\partial v}{\partial t} = A \begin{bmatrix} v \\ p \end{bmatrix} + B \begin{bmatrix} v \\ p \end{bmatrix} - (v \cdot \nabla) v, \qquad x \in \Omega, t > 0, \tag{6a}$$

$$\nabla \cdot v = 0, \qquad x \in \Omega, t > 0, \tag{6b}$$

$$v(\mathbf{x}, 0) = \mathbf{g}'(\mathbf{x}), \qquad x \in \Omega, \tag{6c}$$

$$\text{on the boundary } v(\mathbf{x}, t) = \mathbf{0}, \qquad x \in \partial\Omega, t > 0, \tag{6d}$$

$$\text{and far field condition } \lim_{|\mathbf{x}| \to \infty} v(\mathbf{x}, t) = \mathbf{0}, \qquad t > 0. \tag{6e}$$

Here,

$$A\begin{bmatrix} v \\ p \end{bmatrix} = -(v\cdot\nabla)\bar{v} - (\bar{v}\cdot\nabla)v, \quad x\in\Omega, t>0, \tag{7a}$$

and,

$$B\begin{bmatrix} v \\ p \end{bmatrix} = \left(\frac{1}{Re}\nabla^2 - \frac{\partial}{\partial x}\right)v - \nabla p, \quad x\in\Omega, t>0. \tag{7b}$$

We will devise numerical approximations of the spectra of the operators in equations (7) and compare them with the results of Babenko [3]. $A+B$ is called the linearized Navier-Stokes operator when $\bar{v}$ solves the steady version of equation (5) and the Oseen operator is when $\bar{v} = (1,0)$. The fields (v,p) will be calculated using a similar method used to solve the steady Navier-Stokes system (3).

The novel points of the article are: (1) first ever computational validation of the Babenko spectrum which has been up to this point an entirely theoretical result; (2) computational method to addresses the full exterior domain without truncation; (3) computational simulation of continuous and discrete spectrum; (4) computational algorithm for the spectral problem in exterior domain.

1.1. **Rigorous Results.** The Navier–Stokes system in exterior domains has been studied extensively, see for example Ladyzhenskaya [17], Sritharan [26] or Galdi [12].. All rigorous results in this section are for three dimensions.

Theorem 1. *Oseen operator has a purely continuous spectrum*

$$Spectrum(A+B) = \sigma_c = \left\{\lambda = \alpha + i\beta \in \mathbb{C}, \alpha,\beta\in\mathbb{R}, \alpha + \frac{Re\beta^2}{2} \le 0\right\}. \tag{8}$$

This was shown by Babenko [3, Section 2, Theorem 1] for a single body or a system of bodies. Here $\mathbb{R}$ and $\mathbb{C}$ denotes the space of real and complex numbers respectively. The spectrum is contained in a parabolic tongue that passes through the origin entirely lying in the negative half plane.

Theorem 2. *The spectrum of the linearised Navier–Stokes operator is given by*

$$Spectrum(A+B) = \sigma_c \cup \sigma_p, \tag{9}$$

where σ_c is defined in (8) *and σ_p is a finite number of isolated eigenvalues, whose accumulation points can lie on $\partial\sigma_c$ or at infinity.*

This was shown by Babenko [3, Section 2, Theorem 2] for a single body or for a system of bodies. For background on spectral theory of linear differential operators including those arise in hydrodynamic stability, we refer the reader to Sritharan [26], Yudovich [28] and Richtmyer [23].

2. **Numerical Method**

The eigenvalues were calculated by approximating the eigenfunctions using rational Chebyshev functions in radial direction and Fourier sine-series in the azimuthal direction. The rational Chebyshev function was implemented in two steps, the first step was an algebraic mapping from $r \in [1,\infty)$ into $x \in [-1,1]$ and the second step was the use of Chebyshev polynomials for calculating derivatives in the mapped coordinate system. The mapping used is given by

$$r = L\frac{1+x}{1-x} + 1, \quad r \in [1,\infty), \quad x \in [-1,1], \tag{10}$$

where L is a length parameter. For more information about rational Chebyshev functions, see Boyd [6]. The rational Chebyshev functions was implemented using the collocation method in the radial direction. The derivatives can be calculated using the formulas (see Boyd [6])

$$\frac{\partial}{\partial r} = \frac{Q(x)}{2L}\frac{\partial}{\partial x}, \tag{11a}$$

$$\frac{\partial^2}{\partial r^2} = \frac{Q(x)}{4L^2}\left(Q(x)\frac{\partial^2}{\partial x^2} + 2(x-1)\frac{\partial}{\partial x}\right), \tag{11b}$$

where $Q(x) \triangleq x^2 - 2x + 1$. The matrices used for calculating the derivatives in the computational domain are listed in Peyret [19]. The diagonal elements were calculated using the correction method described by Bayliss et al. [5].

2.1. **Vorticity–Stream Function Formulation.** We solved the following spectral problem for the linearised Navier–Stokes operator

$$-A\begin{bmatrix} v \\ p \end{bmatrix} - B\begin{bmatrix} v \\ p \end{bmatrix} = \lambda v, \tag{12a}$$

$$\nabla \cdot v = 0, \tag{12b}$$

$$\text{on the boundary } v(\mathbf{x},t) = \mathbf{0}, \tag{12c}$$

$$\text{and far field condition } \lim_{|\mathbf{x}|\to\infty} v(\mathbf{x},t) = \mathbf{0}. \tag{12d}$$

By applying the curl to equation system (12) the vorticity–stream function formulation was obtained

$$-\hat{A}\begin{bmatrix} \psi \\ \omega \end{bmatrix} - \hat{B}\begin{bmatrix} \psi \\ \omega \end{bmatrix} = \lambda \omega, \tag{13a}$$

$$\nabla^2 \psi + \omega = 0, \tag{13b}$$

$$\text{on the boundary } \psi = \frac{\partial \psi}{\partial r} = 0, \tag{13c}$$

$$\text{and far field condition } \lim_{r\to\infty} \psi = \lim_{r\to\infty} \omega = 0. \tag{13d}$$

Here,

$$\hat{A}\begin{bmatrix} \psi \\ \omega \end{bmatrix} = -(v\cdot\nabla)\bar{\omega} - (\bar{v}\cdot\nabla)\omega, \tag{14a}$$

$$\hat{B}\begin{bmatrix} \psi \\ \omega \end{bmatrix} = \left(\frac{1}{Re}\nabla^2 - \frac{\partial}{\partial x}\right)\omega, \tag{14b}$$

where the perturbations stream function and vorticity are defined as,

$$\Psi(t) = \bar{\psi} + \psi(t), \quad \Omega(t) = \bar{\omega} + \omega(t) = \nabla\times\bar{v} + \nabla\times v(t). \tag{15}$$

Since Ω is the exterior of the unit disc it is convenient to work with cylindrical coordinate system instead of the Cartesian coordinate system. This means that equations (14) can be written as

$$\hat{A}\begin{bmatrix}\psi\\ \omega\end{bmatrix} = -\left[\frac{1}{r}\frac{\partial\bar{\psi}}{\partial\theta}, -\frac{\partial\bar{\psi}}{\partial r}\right]\cdot\left[\frac{\partial\omega}{\partial r}, \frac{1}{r}\frac{\partial\omega}{\partial\theta}\right] - \left[\frac{1}{r}\frac{\partial\psi}{\partial\theta}, -\frac{\partial\psi}{\partial r}\right]\cdot\left[\frac{\partial\bar{\omega}}{\partial r}, \frac{1}{r}\frac{\partial\bar{\omega}}{\partial\theta}\right], \tag{16a}$$

$$\hat{B}\begin{bmatrix}\psi\\ \omega\end{bmatrix} = \left(\frac{1}{Re}\left(\frac{\partial^2}{\partial r^2} + \frac{1}{r}\frac{\partial}{\partial r} + \frac{1}{r^2}\frac{\partial^2}{\partial\theta^2}\right) - \left(\cos\theta\frac{\partial}{\partial r} - \frac{\sin\theta}{r}\frac{\partial}{\partial\theta}\right)\right)\omega. \tag{16b}$$

The background field $(\bar{v}, \bar{p})$ was calculated using a steady Navier–Stokes equation solver with the same basis and resolution. The details for solving the steady Navier–Stokes equation is in Gustafsson and Protas [14].

2.2. **Discretisation Scheme.** The vorticity and the stream function in equations (13) were discretised in the azimuthal direction using Fourier series

$$\bar{\psi} = \sum_{n=0}^{\infty} \bar{a}_n(r)\sin n\theta, \qquad \theta\in[0,2\pi), r\in[1,\infty), \tag{17a}$$

$$\bar{\omega} = \sum_{n=0}^{\infty} \bar{c}_n(r)\sin n\theta, \qquad \theta\in[0,2\pi), r\in[1,\infty), \tag{17b}$$

$$\psi = \sum_{n=0}^{\infty} a_n(r)\sin n\theta + b_n(r)\cos n\theta, \qquad \theta\in[0,2\pi), r\in[1,\infty), \tag{17c}$$

$$\omega = \sum_{n=0}^{\infty} c_n(r)\sin n\theta + d_n(r)\cos n\theta, \qquad \theta\in[0,2\pi), r\in[1,\infty). \tag{17d}$$

Note that $\bar{\psi}$ and $\bar{\omega}$ are anti–symmetric with respect to the y–axis, while the eigenfunctions are not necessary anti-symmetric. This makes the linear operator (16b) equal to

$$\begin{aligned}\hat{B}\begin{bmatrix}\psi\\ \omega\end{bmatrix} = {} & \frac{1}{Re}\left(\frac{\partial^2}{\partial r^2} + \frac{1}{r}\frac{\partial}{\partial r}\right)\sum_{n=0}^{\infty} c_n(r)\sin n\theta + d_n(r)\cos n\theta \\ & - \frac{1}{Re}\sum_{n=0}^{\infty}\frac{n^2}{r^2}\left(c_n(r)\sin n\theta + d_n(r)\cos n\theta\right) \\ & - \frac{1}{2}\sum_{n=0}^{\infty}\frac{\partial c_n}{\partial r}\left(\sin(n+1)\theta + \sin(n-1)\theta\right) - \frac{n}{r}c_n(r)\left(\sin(n+1)\theta - \sin(n-1)\theta\right) \\ & - \frac{1}{2}\sum_{n=0}^{\infty}\frac{\partial d_n}{\partial r}\left(\cos(n+1)\theta + \cos(n-1)\theta\right) - \frac{n}{r}d_n(r)\left(\cos(n+1)\theta - \cos(n-1)\theta\right).\end{aligned} \tag{18}$$

Equation (13b) in this representation is equal to

$$\begin{aligned}(19)\quad &\left(\frac{\partial^2}{\partial r^2}+\frac{1}{r}\frac{\partial}{\partial r}\right)\sum_{n=0}^{\infty}a_n(r)\sin n\theta+b_n(r)\cos n\theta\\ &-\frac{1}{r^2}\sum_{n=0}^{\infty}n^2(a_n(r)\sin n\theta+b_n(r)\cos n\theta)+\sum_{n=0}^{\infty}c_n(r)\sin n\theta+d_n(r)\cos n\theta=0\end{aligned}$$

By truncating the Fourier series and using a finite number of rational Chebyshev polynomials, we construct a finite dimensional eigenvalue problem. The eigenfunctions should satisfy the correct boundary conditions. In the mapped domain, $x=-1$ is mapped to $r=1$ and $x=1$ is mapped to $r\to\infty$. Since the basis functions do not satisfy all of the boundary conditions, we needed to add rows to the system of equations corresponding to the boundary conditions, for $n=1,2,\ldots,$

$$a_n(1)=b_n(1)=0, \tag{20a}$$

$$\left.\frac{\partial a_n}{\partial r}\right|_{r=1}=\left.\frac{\partial b_n}{\partial r}\right|_{r=1}=0, \tag{20b}$$

$$\lim_{r\to\infty}a_n(r)=\lim_{r\to\infty}b_n(r)=0, \tag{20c}$$

$$\lim_{r\to\infty}c_n(r)=\lim_{r\to\infty}d_n(r)=0, \tag{20d}$$

These equations are needed for no-slip on the cylinders surface, zero radial velocity and zero vorticity at infinity (far field). There is no explicit condition on the azimuthal component of the velocity at infinity as the rational Chebyshev functions already satisfy this condition. Note that there are no boundary condition for vorticity on the surface of the cylinder. Dirichlet boundary conditions can be implemented both at surface of the cylinder and the limit, but Neumann can only be set at the surface of the cylinder ($x=-1$, $r=1$). The spectral basis can not resolve a function which has a Neumann condition at infinity.

2.3. **Numerical Calculations of the Eigenvalues.** The generalised eigenvalue problem was solved using LAPACK command dggevx, see [1]. The algorithm used was **QZ**. Since we used a finite dimensional approximation, spectrum will be purely discrete, see Kreyszig [16]. In order to separate resolved eigenvalues from unresolved eigenvalues, we will use two different resolutions (N_1,N_2) and a range of length scales. If the position of the eigenvalue is the same using both resolutions, then the eigenfunction is resolved and the eigenvalue is accepted. If the position of the eigenvalue changes with resolution the eigenvalue is assumed not to be resolved with the current resolution. We will use the following criteria for accepting an eigenvalue,

$$\delta_j < 5 \cdot 10^{-2}, \quad j = 0, \ldots, N_1. \tag{21}$$

Where L is the length parameter and δ_j is the coordinal difference,

$$\delta_j = \min_{1 \le k \le N_2} \frac{|\lambda_j(N_1) - \lambda_k(N_2)|}{\zeta_j}, \quad j = 0, \ldots, N_1 \tag{22}$$

where,

$$\zeta_1 = |\lambda_1(N_1) - \lambda_2(N_1)|, \tag{23}$$

$$\zeta_j = \frac{1}{2}\left(|\lambda_j(N_1) - \lambda_{j-1}(N_1)| + |\lambda_{j+1}(N_1) - \lambda_j(N_1)|\right), \qquad j > 1. \tag{24}$$

This method is described in detail in [6]. Since we have the option of changing the length parameter L, we can end up with more eigenvalues than N_1. Some of these eigenvalues will be in the same position. Eigenvalues obtained from different resolution are only compared with eigenvalues obtained using the same length scale.

For large Reynolds numbers, the solution to the steady Navier–Stokes equations contains large gradients on the edge of the recirculation zone. Eigenfunctions are expected to have similar behaviour. This makes it hard to numerically resolve the eigenfunctions. Only a few eigenvalues were found for large Reynolds number and the results will not be shown.

3. **Results**

For both the Oseen operator and the linearised Navier–Stokes we used resolution of 70×70 and compared it with resolution 60×60. For the Oseen operator we obtained the parabolic tongue described by Babenko [3]. By varying the length parameter it seems possible to fill the continuous spectrum. For the linearised Navier–Stokes operator, both the continuous part of the spectrum and the point spectrum is obtained. Eigenvalues corresponding to the continuous part spectrum can be obtained for large set of values for the length parameter, while the point spectrum can only be resolved for a narrow range of values for the length parameter.

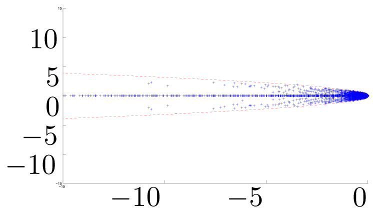

(a) $Re = 2$.

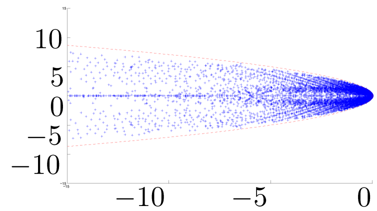

(b) $Re = 10$.

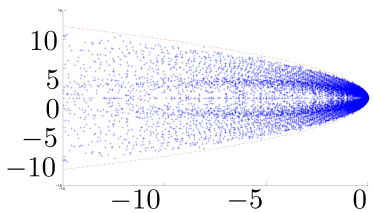

(c) $Re = 20$.

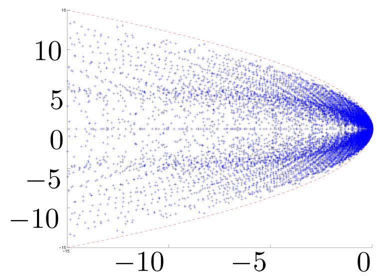

(d) $Re = 30$.

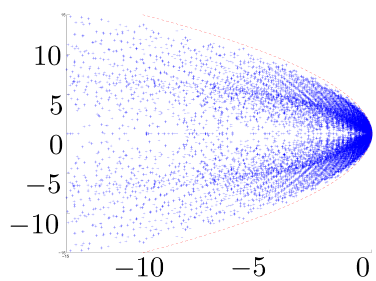

(e) $Re = 40$.

FIGURE 1. Spectrum of the Oseen operator for $2 \leq Re \leq 40$. The calculated eigenvalues are denoted $+$. The dashed line corresponds to the edge of σ_c. All plotted eigenvalues satisfy criteria (21). The resolution was 60×60 and 70×70.

3.1. **Oseen Operator.** The numerical approximation to the spectrum of the Oseen operator is plotted in figure 1. The convex hull of the calculated eigenvalues almost fills the parabolic tongues described in equation (8). The value of the length parameter is either 1, 5, 10 or 15. As the Reynolds number increases the parabolic tongues gets wider. This is the expected behaviour (see equation (8)). While some of the eigenvalues are close to the boundary of the tongue, it seems the eigenvalues accepted by criteria (21) are all inside.

3.2. **Linearised Navier–Stokes Operator.** The spectrum for the linearised Navier–Stokes operator is plotted in figures 2. The spectrum consists of two parts, a parabolic tongue which

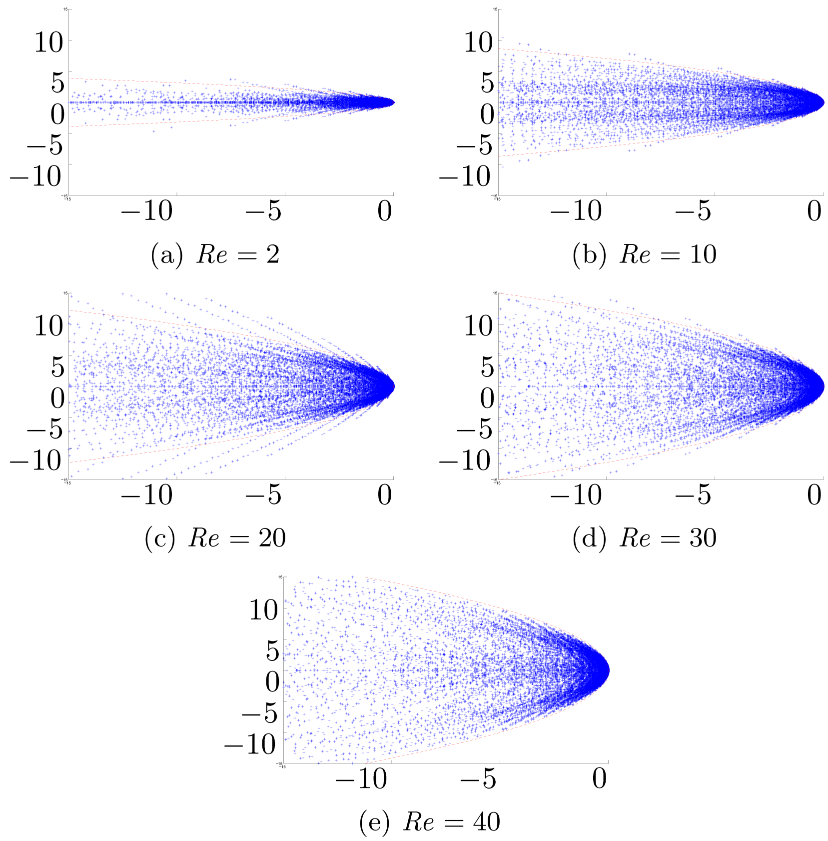

FIGURE 2. Spectrum of the linearised Navier–Stokes operator for $2 \leq Re \leq 40$. The eigenvalues are denoted $+$. The dashed line shows the edge of spectrum σ_c. The resolution was 60×60 and 70×70.

can be described by the Oseen operator σ_c and a set of isolated eigenvalues. The eigenvalues which are outside σ_c were assumed to be the point spectrum described by Babenko [3]. These isolated eigenvalues seem to lay on straight lines starting from the parabolic tongue. For small Reynolds number, less than 20, the eigenvalues belonging to the point spectrum move away from the tongue with increasing Reynolds number. The large Reynolds number, the point spectrum stops moving and the parabolic tongue of the continuous spectrum becomes wider. Some of the eigenvalues of the point spectrum stop being part of the point spectrum and join the continuous part of the spectrum.

4. Conclusions

Spectrum for the Oseen operator and the linearised Navier–Stokes operator were studied using a spectral method with a basis that covers the entire domain exterior to the unit disc. The method can change the location of the collocation points by changing the value of the length parameter. By choosing different values of the length parameter, it is possible to obtain a better approximation to the continuous part of the spectrum. For the Oseen operator, a good numerical approximation of the spectrum described by Babenko [3] was obtained. For the linearised Navier–Stokes operator the numerical method found both the continuous part of the spectrum as well as isolated eigenvalues. By varying the length parameter it is possible to move eigenvalues which are part of the continuous spectrum. The point spectrum is more sensitive to the value of the length parameter and is only resolved for a limited range of values. For operators in unbounded domain which have a spectrum that features a continuous part, the described methods resolve the continuous part of the spectrum well.

Acknowledgements

This research was supported by the Air Force Office of Scientific Research and the Army Research Office Probability and Statistics Program.

Conflict of Interests

The authors declare that there is no conflict of interests.

REFERENCES

[1] E. Anderson, Z. Bai, C. Bischof, S. Blackford, J. Demmel, J. Dongarra, J. Du Croz, A. Greenbaum, S. Hammarling, A. McKenney, and D. Sorensen. LAPACK Users Guide. SIAM, Philadelphia, PA, third edition, 1999.

[2] K. I. Babenko. On the bifurcation of solutions of Navier-Stokes equations. Sov. Phys., Dokl. 25 (1980), 829-831.

[3] K. I. Babenko. Spectrum of the linearized problem of flow of a viscous incompressible liquid round a body. Sov. Phys., Dokl. 27 (1982), 25-27.

[4] V. Barbu and S. S. Sritharan. H^∞-control theory of fluid dynamics. Proc. R. Soc. Lond., Ser. A, Math. Phys. Eng. Sci. 454(1979)(1998), 3009-3033.

[5] A. Bayliss, A. Class, and B. J. Matkowsky. Roundoff error in computing derivatives using the Chebyshev differentiation matrix. J. Comput. Phys. 116(2)(1995), 380 - 383.

[6] J. B. Boyd. Chebyshev and Fourier Spectral Methods. Dover, New York, U.S.A., 2000.

[7] Subrahmanyan Chandrasekhar. Hydrodynamics and Hydromagnetic Stability. Number 1 in Dover Books on Physics Series. Oxford University Press, 1961.

[8] M. Coutanceau and R. Bouard. Experimental determination of the main features of the viscous flow in the wake of a circular cylinder in uniform translation. part 1. steady flow. J. Fluid Mech. 79(2)(1977), 231-256.

[9] E.B. Davies. Spectral Theory and Differential Operators. Number 42 in Cambridge Studies in Advanced Mathematics. Cambridge University Press, 1996.

[10] P. G. Drazin. Hydrodynamic stability. Cambridge University Press, Cambridge, 1981.

[11] Reinhard Farwig and Jir Neustupa. On the spectrum of an oseen-type operator arising from flow past a rotating body. Integral Equations Oper. Theory, 62 (2008), 169-189.

[12] G. P. Galdi. An Introduction to the Mathematical Theory of the Navier- Stokes equations: Linearized Steady Problems, volume 38. Springer-Verlag, 1998.

[13] J. H. Gerrard. The wakes of cylindrical bluff bodies at low Reynolds number. Royal Society of London Philosophical Transactions Series A, 288:351-382, 1978.

[14] Jonathan Gustafsson and Bartosz Protas. Computation of steady incompressible flows in unbounded domains. Comput. Fluids, 112(2015), 94 - 107.

[15] C.P. Jackson. A finite-element study of the onset of vortex shedding in flow past variously shaped bodies. J. Fluid Mech. 182 (1987), 23-45.

[16] Erwin Kreyszig. Introductory functional analysis with applications. Wiley. com, 2007.

[17] O. A. Ladyzhenskaya. The mathematical theory of viscous incompressible flow. Gordon and Breach, New York, 1969.

[18] D. S. Park, D. M. Ladd, and E. W. Hendricks. Feedback control of von Karman vortex shedding behind a circular cylinder at low Reynolds numbers. Phys. Fluids, 6 (7) (1994), 2390-2405.

[19] R. Peyret. Spectral methods for incompressible viscous flow. Springer, New York, first edition, 2002.

[20] Lord Rayleigh O.M. F.R.S. Investigation of the character of the equilibrium of an incompressible heavy fluid of variable density. Proc. Lond. Math. Soc. s1-14 (1) (1882), 170-177.

[21] Lord Rayleigh O.M. F.R.S. LIX. on convection currents in a horizontal layer of fluid, when the higher temperature is on the under side. Phil. Mag. Ser. 6, 32 (192) (1916), 529-546.

[22] Satish C Reddy, Peter J Schmid, and Dan S Henningson. Pseudospectra of the orr-sommerfeld operator. SIAM J. Appl. Math. 53 (1) (1993), 15-47.

[23] R. D. Richtmyer. Principles of Advanced Mathematical Physics, volume 1. Springer-Verlag, 1978.

[24] D. Sattinger. The mathematical problem of hydrodynamic stability. Indiana Univ. Math. J. 19 (1970), 797-817.

[25] P. J. Schmid and D. S. Henningson. Stability and transition in shear flows. Springer, 2001.

[26] S.S. Sritharan. Invariant Manifold Theory for Hydrodynamic Transition. Number 1 in Pitman Research Notes in Mathematics Series. John Wiley & Sons Canada, Limited, 1991.

[27] S. Taneda. Experimental investigation of the wakes behind cylinders and plates at low reynolds numbers. J. Phys. Soc. Japan, 11 (3) (1956), 302-307.

[28] V.I. Yudovich. The Linearization Method in Hydrodynamical Stability Theory. Number 1 in Translations of mathematical monographs. Amer. Math. Soc., 1989.

[29] A. Zebib. Stability of viscous flow past a circular cylinder. J. Eng. Math. 21 (2) (1987), 155-165.